1983ApJ...268..790K

THE ASTROPHYSICAL JOURNAL, 268:790–799, 1983 May 15
© 1983. The American Astronomical Society. All rights reserved. Printed in U.S.A.

ORBITAL PERIOD CHANGES IN CENTAURUS X-3[1]

R. L. KELLEY, S. RAPPAPORT, G. W. CLARK, AND L. D. PETRO
Department of Physics and Center for Space Research, Massachusetts Institute of Technology
Received 1982 June 25; accepted 1982 November 10

ABSTRACT

We present two new times of mid–X ray eclipse for Cen X-3 based on pulse arrival time analyses of pointed observations with *SAS 3*. These results, when combined with all other published eclipse times based on Doppler delay measurements, show that the $2^d.1$ binary period is decreasing at an average rate of $\dot{P}_{\rm orb}/P_{\rm orb} = -1.8\times10^{-6}$ yr^{-1}, but with apparently significant fluctuations about a smooth, linear decrease. The observed changes in the orbital period can be accounted for by mass loss from the system through the L_2 point, although the required rates are implausibly high. We also show that the long-term overall orbital decay can be readily interpreted as the result of torques exerted by the tidally distorted companion star (Krzeminski's star) on the orbiting neutron star. The inferred asynchronism between the orbital frequency and the rotation frequency of the companion star may be maintained by mass and angular momentum loss in a stellar wind, or by a tidal instability related to the Darwin effect. However, this scenario would not provide a natural explanation for any short-term deviations from a constant rate of orbital decay. The implications of an inferred shrinking critical potential lobe around Krzeminski's star are discussed.

Subject headings: stars: binaries — X-rays: binaries

I. INTRODUCTION

The X-ray pulsar Cen X-3 has now been studied for a decade. The early discovery of the binary nature of the source (Schreier *et al.* 1972), identification of the O-type giant companion star (Krzeminski 1974), and determination of the binary system parameters, including the mass of the neutron star (Avni and Bahcall 1974; Bahcall 1978; Rappaport and Joss 1981, and references therein) have made this system the prototype of the massive X-ray–emitting binaries. In addition, the long-term decrease in the 4.8 s pulsation period (Gursky and Schreier 1975; Schreier and Fabbiano 1976) has provided support for the accretion torque model of pulse period changes in X-ray pulsars (Pringle and Rees 1972; Lamb, Pethick, and Pines 1973; Rappaport and Joss 1977; Ghosh and Lamb 1979).

The early *Uhuru* observations indicated that the $2^d.1$ binary period of the system was decreasing at a mean rate of $\dot{P}_{\rm orb}/P_{\rm orb} = -(8\pm4)\times10^{-6}$ yr^{-1} (Schreier *et al.* 1973; Fabbiano and Schreier 1977). Evidence was also presented for a short-term *increase* in the orbital period in 1972 at a rate of $\dot{P}_{\rm orb}/P_{\rm orb} \approx +5\times10^{-4}$ yr^{-1} (Fabbiano and Schreier 1977). Various mass transfer and mass loss effects, as well as tidal interactions, have been considered to explain these changes in the orbital period (van den Heuvel and de Loore 1973; Wheeler, McKee, and Lecar 1974; Sparks 1975; Chevalier 1975; Fabbiano and Schreier 1977; Thomas 1977).

In this paper we present two new precise mid-eclipse time measurements based on pulse arrival time analyses of data taken with *SAS 3* in 1976 November and 1978 December/1979 January. These results are combined with all other available mid-eclipse time measurements determined in the same manner. The data, which span an interval of a decade, indicate that the orbital period of Cen X-3 has continued to decrease, but at about one-fourth the rate suggested by the *Uhuru* measurements, and with apparently significant deviations from a constant rate of decay. We show that the overall period decrease could easily be the result of tidal torques; the inferred asynchronism between the orbit and the rotation of Krzeminski's star could be maintained ultimately by a dynamical instability or by mass and angular momentum loss in a stellar wind. We also explore the effects of angular momentum lost directly from the orbit via mass ejection.

II. *SAS 3* OBSERVATIONS AND RESULTS

Pointed observations of Cen X-3 were carried out with *SAS 3* on several occasions between 1975 and 1979. We have selected the data from two of the observations with the best source exposure: 1976 November 28.4–30.6 and 1978 December 15.3–1979 January 8.8. The second observation lasted for more than 20 days, and the results of detailed studies of the correla-

[1]This work was supported in part by NASA contract NAS5-24441.

© American Astronomical Society • Provided by the NASA Astrophysics Data System

1983ApJ...268..790K

tions between pulse period and X-ray luminosity, as well as eclipse profiles, will be presented elsewhere.

The data recorded with the 3–6 keV energy channel of the horizontal tube detectors (e.g., Buff *et al.* 1977) were selected for the pulse arrival time analyses because of the high counting rate, low background rate, and sufficiently high time resolution (0.416 s). The procedure used to determine the heliocentric pulse arrival times has been described elsewhere (Rappaport, Joss and McClintock 1976; Primini, Rappaport, and Joss 1977). We obtained a total of 59 arrival times for the first observation and 222 for the second. The 1 σ uncertainties in the pulse arrival times were found empirically to be ~ 50 ms for the first observation and ~ 30 ms for the second.

For the 1976 observation we computed minimum χ^2 fits of the pulse arrival times to a function that includes the Doppler delays due to a circular orbit and the time delays due to a constant rate of change of pulse period. The free parameters in the fit were the projected semi-major axis of the neutron star orbit, $a_x \sin i$, time of mid–X-ray eclipse (for an assumed circular orbit), T_e, pulse period, P, pulse phase reference, and rate of change of intrinsic pulse period, $\dot{P}$. The value of the orbital period was held fixed at $P_{\rm orb} = 2^{\rm d}.087117$ (Table 3). The best-fit values of the parameters are listed in Table 1 along with formal 1 σ confidence limits.

The behavior of the intrinsic pulse period during the course of the 1978–1979 observation was sufficiently complex that even a relatively high-order polynomial in time plus a circular orbit did not adequately fit the pulse arrival times over the entire 20 day observation. To improve the fits, we divided the data set into two nearly equal segments and fitted a common binary orbit to the entire set while simultaneously fitting a different low-order polynomial in time to each segment (see, e.g., Kelley, Rappaport, and Petre 1980). It was found that the best-fit orbital parameters ($a_x \sin i$, T_e, and $P_{\rm orb}$) were not very sensitive to the choice of the order of these polynomials. This is to be expected since the data contain 10 cycles of the binary orbit, and the orbital Doppler delays are essentially uncorrelated with the intrinsic pulse period behavior. The resulting best-fit orbital parameters obtained by this procedure are also listed in Table 1; the corresponding Doppler delay curve is shown in Figure 1, along with the residuals from the fit. The pulse period behavior for the 1978–1979 observation is dominated by an overall spin-up of $\dot{P}/P = -5.3 \times 10^{-4}$ yr^{-1}. This is about a factor of 2 greater than the observed long-term spin-up rate (see, e.g., Rappaport and Joss 1982).

We also carried out eccentric-orbit fits to the arrival times from the 1978–1979 observation. Only a marginally significant detection of the orbital eccentricity, $e = 0.0004 \pm 0.0002$, was obtained, which is just barely consistent with the value of $e = 0.0008 \pm 0.0001$ determined by Fabbiano and Schreier (1977).

To study possible changes in the orbital period, we have collected all available mid-eclipse times and the corresponding uncertainties determined from X-ray pulse timing analyses (Table 2). The deviations in mid-eclipse times from those predicted for a constant orbital period are shown in Figure 2 (these are hereafter referred to as mid-eclipse time delays). Statistically significant and systematic variations of up to ~ 800 s are apparent; the *reduced* χ^2 for a fit to a constant orbital period is 624 (per degree of freedom) for 22 degrees of freedom. When a quadratic function is fitted to the mid-eclipse times, the reduced χ^2 is found to be 30 (per degree of freedom) for 21 degrees of freedom. Thus, the addition of a quadratic term leads to a very substantial improvement in the fit, but there still remain statistically significant deviations. The best-fit quadratic function is shown in Figure 2.

Before discussing the possibility that the observed mid-eclipse time delays result from a changing orbital period, we caution that the eclipse-time measurements (and their uncertainties) in Figure 2 are from a number of different satellite experiments, and thus were not necessarily determined by a uniform analysis procedure.

TABLE 1

CIRCULAR ORBIT FITS TO SAS 3 PULSE ARRIVAL TIME DATA FROM CENTAURUS X-3[a]

Parameter	Observation 1 1976 Nov	Observation 2 1978 Dec–1979 Jan
$a_x \sin i$	39.549 ± 0.027 lt-sec	39.636 ± 0.003 lt-sec
T_e	JD 2,443,112.76642 $\pm$ 0$^{\rm d}$.00040	JD 2,443,870.38910 $\pm$ 0$^{\rm d}$.00002
$P_{\rm orb}$	2$^{\rm d}$.087117[b]	2$^{\rm d}$.087097 $\pm$ 0$^{\rm d}$.000008
P[c]	4.8336641 ± 0.0000015 s	4.8335959 ± 0.0000001 s
$\dot{P}/P$	$< 7 \times 10^{-4}$ yr^{-1}	$\sim -5.3 \times 10^{-4}$ yr^{-1}

[a]All quoted uncertainties are single-parameter 1 σ confidence limits.
[b]Held fixed at this value (see Table 3).
[c]Heliocentric pulse period referred to an epoch of JD 2,443,112.0 for observation 1 and JD 2,443,867.0 for observation 2.

© American Astronomical Society • Provided by the NASA Astrophysics Data System

1983ApJ...268..790K

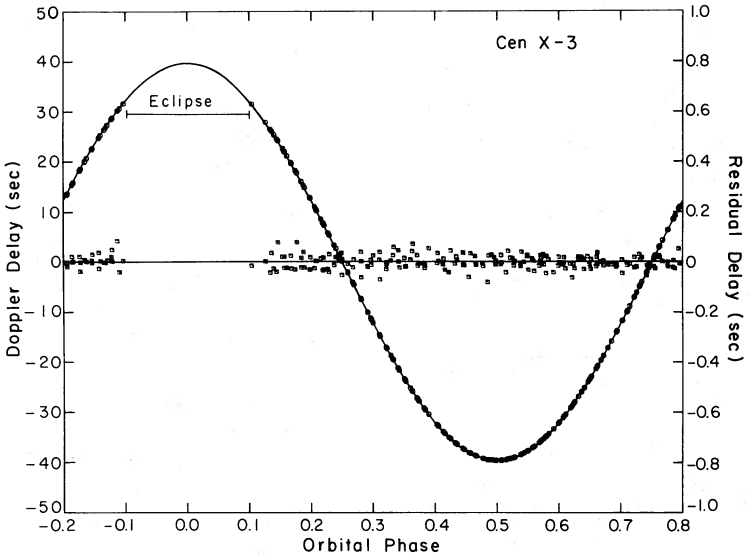

FIG. 1.—Cen X-3 Doppler delay data from *SAS 3* observations in 1978 December–1979 January. Solid curve represents the best-fit circular orbit (Table 1). Points clustered around zero Doppler delay (*small squares*) are the residuals of the data points from the best-fit orbit. Note that the scale for the residuals (*right-hand ordinate*) is 50 times that for the Doppler delays.

TABLE 2

CENTAURUS X-3 ECLIPSE TIMES[a]

Orbital Cycle	Time JD − 2,440,000.0	Reference
0	$958.84643 \pm 0^{d}00045$	Fabbiano and Schreier 1977
57	1077.81497 ± 0.00015	Fabbiano and Schreier 1977
83	1132.08181 ± 0.00029	Fabbiano and Schreier 1977
91	1148.78051 ± 0.00016	Fabbiano and Schreier 1977
166	1305.31533 ± 0.00014	Fabbiano and Schreier 1977
273	1528.64010 ± 0.00030	Fabbiano and Schreier 1977
284	1551.59798 ± 0.00017	Fabbiano and Schreier 1977
293	1570.38199 ± 0.00011	Fabbiano and Schreier 1977
295	1574.55610 ± 0.00013	Fabbiano and Schreier 1977
296	1576.64330 ± 0.00010	Fabbiano and Schreier 1977
297	1578.73037 ± 0.00007	Fabbiano and Schreier 1977
298	1580.81722 ± 0.00009	Fabbiano and Schreier 1977
300	1584.99193 ± 0.00010	Fabbiano and Schreier 1977
303	1591.25328 ± 0.00015	Fabbiano and Schreier 1977
304	1593.34025 ± 0.00015	Fabbiano and Schreier 1977
307	1599.60212 ± 0.00015	Fabbiano and Schreier 1977
308	1601.68930 ± 0.00014	Fabbiano and Schreier 1977
309	1603.77671 ± 0.00021	Fabbiano and Schreier 1977
709	2438.628 ± 0.003	Tuohy 1976
876	2787.1755 ± 0.0007	van der Klis, Bonnet-Bidaud, and Robba 1980
1032	3112.76642 ± 0.0004	This work
1314	3701.33275 ± 0.00043	Howe *et al.* 1982
1395	3870.38910 ± 0.00002	This work
1786	4686.44760 ± 0.00005	Murakami *et al.* 1982

[a]Eclipse times are based on circular orbit fits to pulse arrival times.

© American Astronomical Society • Provided by the NASA Astrophysics Data System

1983ApJ...268..790K

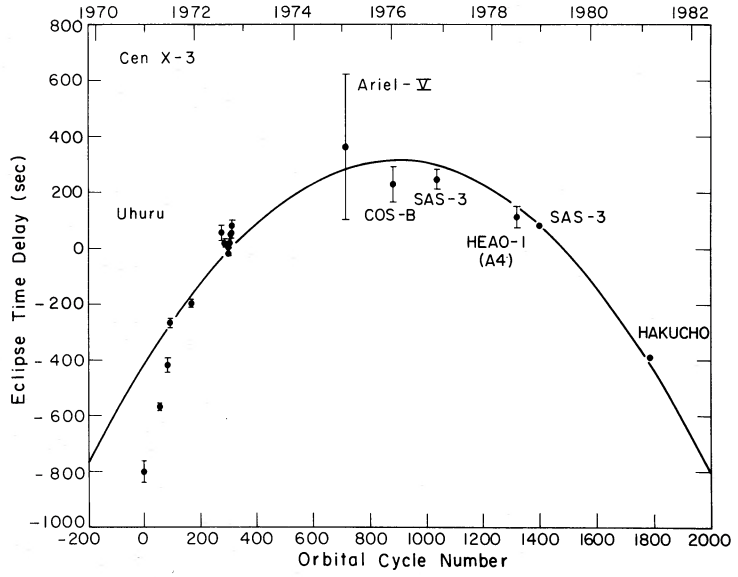

FIG. 2.—Cen X-3 mid X-ray eclipse time delays. The observed-minus-calculated eclipse times are plotted with respect to the ephemeris t_n = JD 2,440,958.8557 + 2^d.0871201 n. The eclipse times and references are given in Table 2. Solid curve represents the best-fit to a constant rate of orbital decay ($\dot{P}_{orb}/P_{orb} = -1.8 \times 10^{-6}$ yr^{-1}).

Although this might account for some of the nonstatistical deviations from the best-fit quadratic function, the overall systematic trend of the mid-eclipse time delays apparent in Figure 2 must certainly be real.

We further note that if the orbit of Cen X-3 is eccentric, with $e = 0.0008$ (Fabbiano and Schreier 1977), simple sinusoidal fits to the Doppler delay data will, in general, not yield the true mid-eclipse times (Deeter, Boynton, and Pravdo 1981). In this type of analysis, systematic, periodic deviations from the true eclipse times of up to $eP_{orb}/2$ (cf. Thomas 1974) may result if apsidal motion is present in the system. However, this time difference is smaller than ~ 100 s for the Cen X-3 system, and therefore cannot explain the observed variations in the eclipse delays (Fig. 2). Furthermore, the "eclipse times" determined from sinusoidal fits have the advantage that they yield the *mean* orbital period, regardless of the observation interval, even if apsidal motion is present in an eccentric binary system. This is to be expected since the first term in the Fourier expansion of the orbital Doppler delays contains no information about the eccentricity. We therefore continue to use the term "mid-eclipse times" even though, strictly speaking, the actual eclipse times for an eccentric orbit cannot be determined from circular orbit fits.

A constant rate of change of the orbital period will lead to a quadratic variation in the mid-eclipse time delays. The time of the nth mid-eclipse is then given by

$$t_n \approx t_0 + P_{orb} n + 1/2 P_{orb} \dot{P}_{orb} n^2, \quad (1)$$

where P_{orb} and $\dot{P}_{orb}$ are the orbital period and its derivative, respectively, at time t_0. From the best-fit quadratic function and equation (1) we obtain $\dot{P}_{orb}/P_{orb} = -(1.8 \pm 0.1) \times 10^{-6}$ yr^{-1}. (The uncertainty was determined after scaling up the error bars on the individual measurements until χ^2 per degree of freedom equaled unity.) The value of $\dot{P}_{orb}/P_{orb}$ that we obtain is about one-fourth the value determined by Fabbiano and Schreier (1977), who used a shorter data span, although it is formally consistent with their 2 σ result. The orbital period ephemeris implied by our best-fit values of t_0, P_{orb}, and $\dot{P}_{orb}$ is given in Table 3.

When carrying out χ^2 fits to a series of data points obtained in different experiments, with error bars that differ greatly, and where nonstatistical deviations are clearly evident, it is often instructive to carry out an additional fit where all data points are weighted equally. Such a comparative test provides a measure of the

TABLE 3

LONG-TERM ORBITAL PERIOD BEHAVIOR OF CENTAURUS X-3

Time of the nth mid-X-ray eclipse and orbital period:

$$t_n = t_0 + P_{orb} n + 1/2 P_{orb} \dot{P}_{orb} n^2$$
$$P_{orb}(t) = P_{orb} + \dot{P}_{orb}(t - t_0)$$

t_0 = JD 2,440,958.8509 ± 0^d.0003
P_{orb} = 2^d.0871390 ± 0^d.0000009
$1/2\, P_{orb} \dot{P}_{orb} = -(1.06 \pm 0.05) \times 10^{-8}$ days
$\dot{P}_{orb} = -(1.02 \pm 0.05) \times 10^{-8}$
$\dot{P}_{orb}/P_{orb} = -(1.78 \pm 0.08) \times 10^{-6}$ yr^{-1}
Standard deviation of the 24 measured eclipse times from t_n = 105 s

© American Astronomical Society • Provided by the NASA Astrophysics Data System

1983ApJ...268..790K

dependence of the fitted parameter values on the details of the assigned error bars. We have, therefore, also carried out a χ^2 fit in which equal uncertainties are assigned to each mid-eclipse time measurement. In this case we obtain only a slightly larger value for $\dot{P}_{\rm orb}/P_{\rm orb}$ than obtained above: $\dot{P}_{\rm orb}/P_{\rm orb} = -(2.2 \pm 0.2) \times 10^{-6}$ yr^{-1}, where the error bar is again a formal statistical uncertainty.

Finally, we comment on the deviations of the eclipse times from a simple quadratic fitting function (corresponding to a uniform orbital decay rate). These observed deviations (Fig. 2) indicate that there are apparently intervals when the decay rate is faster than the average and other intervals when the decay rate is slower than average. Nonetheless, all the eclipse times seem to be consistent with an orbital *decay*, with the possible exception of the cluster of *Uhuru* measurements (Fabbiano and Schreier 1977) around orbital cycle 300. A formal fit to the 13 eclipse times in the subgroup of the data yields an orbital *expansion* rate corresponding to $\dot{P}_{\rm orb}/P_{\rm orb} = +(4 \pm 1) \times 10^{-4}$ yr^{-1} (also see Fabbiano and Schreier 1977). If the published uncertainties for these eclipse times are accepted at "face value," then orbital expansion has been observed at the 4 σ confidence level. However, we note that the corresponding values of $a_x \sin i$ (Fabbiano and Schreier 1977) show an empirical scatter of ~ 57 ms about the mean, in contrast to the quoted uncertainty of ~ 23 ms. We therefore conclude that the quoted uncertainties in eclipse times are also likely to have been underestimated by the same factor of ~ 2. If the 13 eclipse times near cycle 300 are reanalyzed with error bars enlarged by a factor of ~ 2, the statistical significance of the short-term, rapid orbital expansion is greatly diminished. We obviously cannot be certain that the orbit did not expand; however, we will focus attention in the remainder of this paper only on the highly significant long-term orbital decay.

III. DISCUSSION

The rate of change of the orbital period of a binary system is determined primarily by considerations of angular momentum. In particular, there are two principal ways in which the orbital angular momentum of the stellar components may change. The first involves the loss of mass from at least one of the components; this might take place by critical-potential lobe overflow or by a stellar wind. Even if the total mass and total angular momentum of the binary system remain constant during mass transfer, the orbital period will, in general, change due to the redistribution of the angular momentum. If mass is lost from the binary system, it is likely to carry away angular momentum. In this case there are a number of possible modes by which angular momentum can be transported away. For example, the matter may escape from the L_2 point following Roche lobe overflow, or be ejected in the wind of a rotating star.

The second way in which orbital angular momentum can be modified is through a tidal interaction. Here, one or both of the members of a close binary system will be tidally distorted, and, through viscous forces, the tides raised on one star will lag (or lead) the other orbiting component as long as the stellar rotation is not synchronous with the orbit. A torque is thus exerted which tends to decrease (or increase) the orbital angular momentum. This mechanism accounts for the presently increasing orbital period in the Earth-Moon system (see, e.g., Darwin 1879; Counselman 1973).

In the discussion that follows, we consider both of these processes in detail and show that with plausible assumptions, the observed overall orbital period decrease of the Cen X-3 system is probably ultimately produced by tidal coupling of Krzeminski's star to the orbiting neutron star.

In a binary system consisting of two *point masses*, M_c (the companion star) and M_x (the X-ray star), the orbital angular momenta of the two components are related by $L_x = L_c (M_c/M_x)$. If mass transfer and mass loss occur, the rate of change of L_x, and hence the effective torque on the orbiting X-ray star (if the orbit is assumed to remain circular), is given by

$$\dot{L}_x = L_c \frac{\dot{M}_c}{M_c} \left(\frac{1 + \beta/q}{1+q} \right) + \dot{L}_T \left(\frac{1}{1+q} \right), \qquad (2)$$

where $L_T = L_x + L_c$ is the total orbital angular momentum, $q = M_x/M_c$, and β is the fraction of mass lost by M_c that is captured by M_x ($\beta = -\dot{M}_x/\dot{M}_c$). The first term on the right side of equation (2) represents the torque due to mass transfer, and the second term is the torque due to mass and angular momentum loss from the system. If the mass transfer process is conservative in both total mass and angular momentum, then $\beta = 1$ and $\dot{L}_T = 0$.

For mass transfer processes that are not conservative, the rate at which angular momentum is lost from the system must be specified. A convenient way to parameterize this rate is to take

$$\dot{L}_T = \xi \dot{M}_T a_c^2 \omega_K = \xi \dot{M}_c (1-\beta) a_c^2 \omega_K, \qquad (3)$$

where ξ is a dimensionless parameter that is to be specified or determined, M_T is the total mass of the binary, a_c is the semimajor axis of the orbit of the mass losing star, and ω_K is the orbital angular velocity. We define a torque on the orbiting neutron star due to mass loss and exchange by $N_x^{\dot{m}} \equiv \dot{L}_x$. With the above definition of $\dot{L}_T$ we can rewrite equation (2):

$$N_x^{\dot{m}} = \dot{M}_c a^2 \omega_K \left\{ \frac{[1 + \beta/q + \xi(1-\beta)] q^2}{(1+q)^3} \right\}. \qquad (4)$$

We emphasize that equation (4) is an approximate,

© American Astronomical Society • Provided by the NASA Astrophysics Data System

1983ApJ...268..790K

parameterized expression that we expect will effectively incorporate all of the complex interactions of matter during transfer and loss from the system, including the effects of a possible disk that may mediate the accretion onto the neutron star.

In the case of the Cen X-3 system, the moment of inertia of the companion star is $0.50 \pm {}^{0.82}_{0.18}$ (95% confidence[2]) times the moment of inertia of the orbit ($a^2 M_x M_c / M_T$), and thus can not be neglected in the orbital dynamics. In this case we expect that equation (4) will continue to be valid, with ξ still defined as the *orbital* angular momentum lost from the binary system per unit mass lost. If rotational angular momentum is carried away from the companion star at a significant rate via a stellar wind, then the rate of *total* angular momentum loss may be considerably larger than that lost directly from the orbit. However, this will not affect the orbit until tidal torques couple the two components (see discussion below).

To account explicitly for the tidal interaction, we have adopted a simple one-parameter expression for the tidal torque on the orbiting neutron star due to a tidal lag:

$$N_x^t = - I_c \frac{(\omega_K - \omega_c)}{\tau}, \tag{5}$$

where I_c is the moment of inertia of the companion, ω_c is its angular frequency, and τ is a synchronization time scale (which, for radiatively damped dynamical tides [Zahn 1977], is itself a function of $\omega_K - \omega_c$). Equation (5), in its simplist form, is based on the notion that the tidal lag angle is expected to be approximately proportional to the difference in angular velocities between the companion star and the orbit (see, e.g., Lecar, Wheeler, and McKee 1976; Zahn 1977, and references therein).

The dynamical equations governing the evolution of the system are given by

$$\frac{dJ_c}{dt} = N_c^t + N_c^{\dot{m}}, \tag{6a}$$

$$\frac{dJ_x}{dt} = N_x^t + N_x^{\dot{m}}. \tag{6b}$$

In these expressions J_c and J_x are now the total angular momenta (i.e., rotational plus orbital) of the companion star and the neutron star with respect to the center of mass of the binary system, and $N_c^{\dot{m}}$ and N_c^t are the mass-loss and tidal torques, respectively, on the companion star. The spin angular momentum of the *neutron star* in the Cen X-3 system is much smaller than the orbital angular momentum and thus can be neglected in equation (6b) (i.e., $J_x \approx L_x$). The orbital period derivative can be computed from equations (4), (5), (6b), and Kepler's third law, $a^3 \omega_K^2 = G M_T$:

$$\frac{\dot{P}_{\rm orb}}{P_{\rm orb}} = 3f \frac{\dot{M}_c}{M_c} - 3g \left(\frac{\omega_K - \omega_c}{\omega_K} \right) \frac{1}{\tau}, \tag{7a}$$

where

$$f = \beta/q - \frac{2/3 + \beta/3 + q[1 - \xi(1-\beta)]}{(1+q)}, \tag{7b}$$

and

$$g = \eta (1+q)^2 (R_c/a)^2 / q. \tag{7c}$$

The quantity η is the moment of inertia of the companion star in units of $M_c R_c^2$. Equation (7) is significantly different from the expressions for $\dot{P}_{\rm orb}/P_{\rm orb}$ given by Fabbiano and Schreier (1977) and Thomas (1977) in that it has been derived by considering only the torque on the orbiting neutron star, rather than the net torque on the entire binary system. The advantage of this approach is that it does not require any assumptions about the time rate of change of both the radius and angular velocity of the companion star. We emphasize, however, that equation (7) yields only the *instantaneous* value of the rate of change of the orbital period. To determine the evolution of the orbital period and the other orbital parameters requires a solution of the coupled differential equations (6a,b).

To investigate the implications of equation (7), we consider two limiting cases: (i) the synchronization time scale is much longer than the time scale for orbital decay ($P_{\rm orb}/\dot{P}_{\rm orb} \approx 5 \times 10^5$ yr), and the orbital period changes are therefore due entirely to the effects of mass loss and exchange, and (ii) tidal effects dominate the orbital dynamics.

The relation between the X-ray luminosity, L_x, and the mass accretion rate, $\dot{M}_x$, provides an additional constraint on the mass loss rate:

$$\frac{\dot{M}_c}{M_c} = - \frac{1}{\beta} \left(\frac{R_x L_x}{G M_c M_x} \right), \tag{8a}$$

or, for the parameters of Cen X-3 given below,

$$\dot{M}_c \approx -6 \times 10^{-9} \frac{1}{\beta} \left(\frac{L_x}{5 \times 10^{37} \text{ ergs s}^{-1}} \right) M_\odot \text{ yr}^{-1}. \tag{8b}$$

(We have assumed here that the time delay between mass loss by the companion and accretion onto the

[2] The value for the moment of inertia of Krzeminski's star and the corresponding uncertainty were obtained from a Monte Carlo error propagation technique (Rappaport, Joss, and Stothers 1980; Rappaport and Joss 1982) and from calculations of the moment of inertia [$I = (0.06 \pm 0.02) M_c R_c^2$] of stars similar to Krzeminski's star by Stothers (1982).

© American Astronomical Society • Provided by the NASA Astrophysics Data System

1983ApJ...268..790K

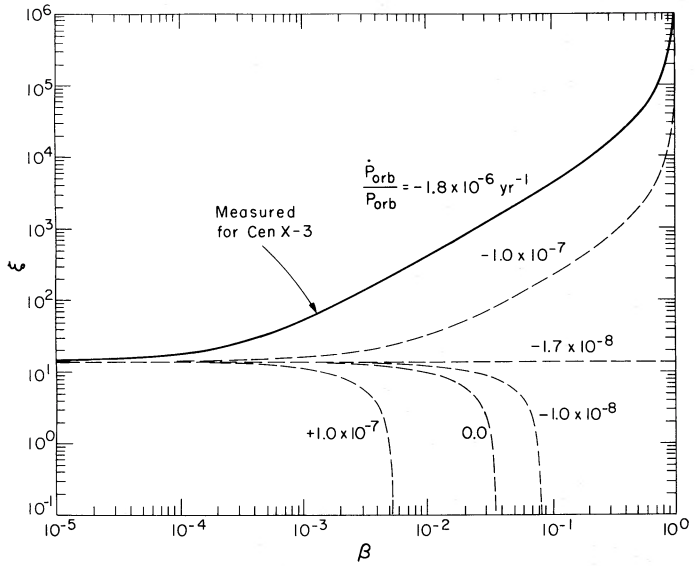

FIG. 3.—Angular momentum loss parameter, ξ, vs. mass capture fraction, β (see eq. [7]). Solid curve gives the relation between ξ and β for the case that mass and angular momentum loss from the Cen X-3 system account for the observed orbital period changes. Dashed curves indicate illustrative values of ξ and β that would result in different rates of change in the orbital period (including positive values of P_{orb}). These curves are calculated for the orbital parameters and the X-ray luminosity of the Cen X-3 system.

neutron star surface is negligible compared to the time scale for changes in the orbital period.) To explore the effects of case (i) (mass-loss dominated orbital dynamics) we combine equations (7) and (8) with $\tau \to \infty$ and obtain a relation between the orbital angular momentum loss parameter ξ and the mass capture fraction, β. This relation is shown as the solid curve in Figure 3. In plotting this relation, we have taken $M_x = 1.0$ $M_\odot$, $M_c = 19.0$ $M_\odot$, $R_x = 10$ km, and $L_x = 5 \times 10^{37}$ ergs s^{-1} (see, e.g., Rappaport and Joss 1981; 1982), and $\dot{P}_{orb}/P_{orb} = -1.8 \times 10^{-6}$ yr^{-1} (see § II).

Inspection of Figure 3 reveals that the minimum value of the orbital angular momentum loss parameter, ξ, that can yield the observed orbital decay rate is ~ 14. This minimum value of ξ is attained as $\beta \to 0$ (i.e., most of the mass lost by the companion is ejected from the system). For capture fractions in the range $10^{-4} \lesssim \beta \lesssim 10^{-3}$, values of ξ in the range 20–50 are required to explain the observed orbital decay. Thus, we see that the *orbital* angular momentum carried away per unit mass loss must be considerably larger than the specific orbital angular momentum of the companion (i.e., $\xi \gg 1$; see also Fabbiano and Schreier 1977). The dashed curves in Figure 3 illustrate the relation between ξ and β for smaller values of the rate of decay of the orbital period. Note, in particular, that for ξ and β sufficiently small the orbital period will actually increase. Furthermore, for conservative mass transfer ($\dot{P}_{orb}/P_{orb} = -1.7 \times 10^{-8}$ yr^{-1} with $\beta = 1$) we see that $\dot{P}_{orb}/P_{orb}$ is two orders of magnitude smaller than that observed for Cen X-3.

Large values of ξ could be attained if the characteristic "lever arm" for the ejected matter were closer in size to the full semimajor axis, a, rather than to the value of a_c as used in equation (3). This might seem a more reasonable choice for the case of mass loss via a moderately high-velocity stellar wind, since the specific angular momentum of matter at the surface of a nearly corotating companion (and hence that of the stellar wind) would be significantly larger (by a factor $[R_c/a_c]^2 \approx 150$) than that implied by equation (3). As discussed above, however, this angular momentum comes from the *rotational* angular momentum of the companion and not directly from the orbit, unless there is the appropriate coupling by tidal torques (see discussion below). In addition, we note that in the Cen X-3 system, the expected capture fraction from a high-velocity stellar wind is $\beta \lesssim 10^{-3}$ (Davidson and Ostriker 1973; Lamers, van den Heuvel, and Petterson 1976; Bonnet-Bidaud and van der Klis 1979). This implies (from eq. [8b]) that $\dot{M}_c \gtrsim 6 \times 10^{-6}$ $M_\odot$ yr^{-1}, which is at the high end of the range of the stellar wind mass loss rates expected for a star of spectral type O6–8f (Hutchings *et al.* 1979): $\sim 2 \times 10^{-7}$–6×10^{-6} $M_\odot$ yr^{-1} (Abbott *et al.* 1980; Garmany *et al.* 1981; Lamers 1981).

A mass-loss mode that could yield a large value of ξ ($\gtrsim 10^2$) would occur if much of the matter leaving Krzeminski's star escaped via Roche lobe overflow followed by loss from the system through the L_2 point. The corresponding mass capture fraction, from Figure 3, is $\beta \approx 2 \times 10^{-3}$. In this picture, matter flows through the

© American Astronomical Society • Provided by the NASA Astrophysics Data System

1983ApJ...268..790K

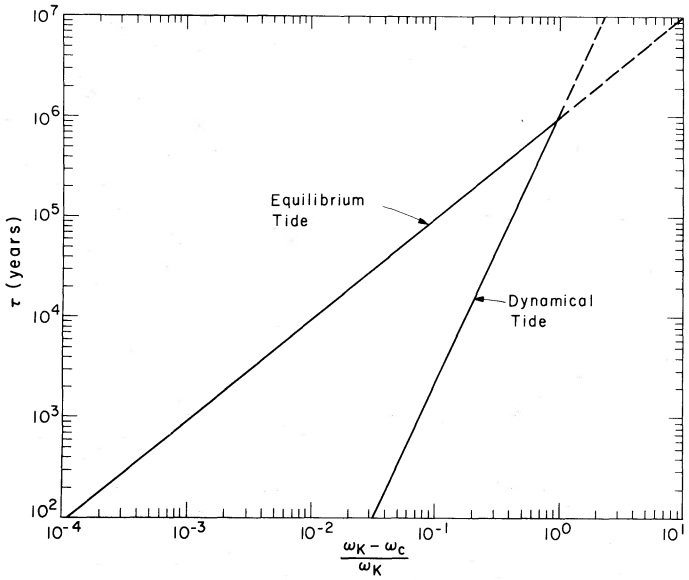

FIG. 4.—Relation between the synchronization time scale, τ, and the synchronism parameter, $\gamma = (\omega_K - \omega_c)/\omega_K$, required to explain the observed rate of decrease in the orbital period of Cen X-3. Synchronism corresponds to $\gamma = 0$, the tidal case to $\gamma = 1$, and counter-rotation to $\gamma > 1$. The curves labeled "equilibrium tide" and "dynamical tide" are plots of eqs. (7a) and (10), respectively, with $f = 0$ (pure tidal interaction), and $P_{\rm orb}/P_{\rm orb} = -1.8 \times 10^{-6}$ yr^{-1}.

inner Lagrange point at a rate of $\sim 3 \times 10^{-6}\ M_\odot$ yr^{-1} (see eq. [8b]) with only a small fraction captured by the neutron star. This much matter flowing in a relatively thin disk or streamlike structure with a typical velocity of a few hundred km s^{-1} could result in densities in excess of 10^{14} cm^{-3} and column densities of up to 10^{26} cm^{-2}. It seems highly unlikely that such a stream of matter would have gone undetected in orbital phase dependent X-ray and optical studies. In fact, column densities of only $\sim 5 \times 10^{23}$ cm^{-2} are required to produce the observed intensity dips at orbital phase ~ 0.6 (Pounds *et al.* 1975; Jackson 1975; Schreier *et al.* 1976) and the extended OFF states due to "choking" (Giacconi 1975; Schreier *et al.* 1976). We therefore tentatively discount this mode of mass transfer for driving the orbital decay, although we cannot completely rule out the possibility that we are viewing the system at just the right inclination to observe broad eclipses while avoiding the obscuration effects of such large matter flows.

From the above discussion we conclude that the loss of matter and concomitant orbital angular momentum loss from the Cen X-3 system is probably insufficient *by itself* (i.e., in the absence of tidal effects) to explain both the magnitude and sign of the overall long-term orbital period changes (see discussions in van den Heuvel and de Loore 1973; Wheeler, McKee, and Lecar 1974; Sparks 1975; Chevalier 1975; Fabbiano and Schreier 1977; Thomas 1977).

The effects of the tidal interaction given by equation (5) can be assessed by examining equation (7) with f set equal to zero. In this case we obtain a simple relation between the degree of asynchronism, $(\omega_K - \omega_c)/\omega_K$, and the synchronization time scale, τ. This is shown graphically in Figure 4. For this result we have again used $\dot{P}_{\rm orb}/P_{\rm orb} = -1.8 \times 10^{-6}$ yr^{-1}, $R_c/a = 0.65$ (Rappaport and Joss 1982), and adopted a value for $\eta = 0.06$ (see footnote [2]). As an example, it is found that the observed orbital period decrease can be accounted for with a synchronization time scale of $\sim 10^5$ yr if the system is out of corotation by only 10%. The dashed portion of the curve in Figure 4 corresponds to a sense of rotation of the companion star that is opposite to that of the orbital motion.

Zahn (1975, 1977) gives an expression for the tidal torque for the case of radiatively damped dynamical tides (see also Nicholson 1979 for a more recent study of dynamical tides). When Zahn's (1977) equation (5.6) is cast in the form of our equation (5) it reads:

$$N_x^t = -I_c \frac{(\omega_K - \omega_c)}{\tau_D} \left(\frac{\omega_K - \omega_c}{\omega_K} \right)^{5/3}, \qquad (9a)$$

where

$$\tau_D^{-1} = 3 \times 2^{5/3} \left(\frac{GM_c}{R_c^3} \right)^{1/2} \left(\frac{R_c}{a} \right)^{17/2} \eta^{-1} q^2 (1+q)^{5/6} E_2, \qquad (9b)$$

and E_2 is Zahn's tidal coefficient. Our definition of τ_D is

© American Astronomical Society • Provided by the NASA Astrophysics Data System

1983ApJ...268..790K

the same to within a factor 5/3 of Zahn's $t_{\rm sync}$ (1977; eq. [5.7]). Equation (7a) (with $f = 0$) then becomes

$$\frac{\dot{P}_{\rm orb}}{P_{\rm orb}} = -3g\left(\frac{\omega_K - \omega_c}{\omega_K}\right)^{8/3}\frac{1}{\tau_D}. \quad (10)$$

This equation yields a simple relation between τ_D and $(\omega_K - \omega_c)/\omega_K$, which is also plotted in Figure 4. The numerical value of E_2 for a star like Krzeminski's star is probably in the range 3×10^{-6}–1×10^{-5} (Zahn 1975, 1977). Thus, we see from equation (9b) that τ_D should lie in the range $\sim 4\times10^3$–1×10^4 yr. From Figure 4 we can then infer a value of $\sim 20\%$ for $(\omega_K - \omega_c)/\omega_K$.

From the above discussion we see that it is quite plausible that the observed long-term orbital period decrease could be due largely to tidal effects. *It is unclear, however, whether the apparent deviations from a constant rate of orbital decay can find a natural explanation in the context of tidal interactions.*

Theoretical calculations indicate that in many cases the synchronization time scale in X-ray binaries should be of the same order of (or shorter than) the circularization time scale (Lecar, Wheeler, and McKee 1976; Zahn 1977; Hut 1981). One might then wonder why Krzeminski's star, which is in a highly circular orbit (Fabbiano and Schreier 1977), would not rotate synchronously with the orbit. There are at least two distinctly different mechanisms that can account for such asynchronism and hence the tidal torque effects. The first invokes angular momentum loss in a stellar wind. The specific angular momentum of material at the surface of Krzeminski's star is $\sim R_c^2\omega_c$. With a stellar wind mass loss rate of $\sim 6\times10^{-6}\ M_\odot\ {\rm yr}^{-1}$, the angular momentum carried away in the wind would be sufficient to explain the orbital decay rate. In this mode, the companion would continuously lose rotational angular momentum to its stellar wind and, through the action of tidal torques, extract angular momentum from the orbit.

The second scenario invokes a self-generating tidal instability of the basic type originally proposed by Darwin (1879) and explored more recently by Counselman (1973), van Hamme (1979), and Hut (1980, 1981). As discussed earlier, the moment of inertia of Krzeminski's star (about its center of mass) is $0.50 \pm {}^{0.82}_{0.18}$ times the moment of inertia of the binary system. Darwin (1879) showed that, for the case of a binary system where the component *masses and radii are constant* in time, the equilibrium configuration with $\omega_K = \omega_c$ will be secularly unstable if the rotational angular momentum of the companion is larger than one-third the total orbital angular momentum. Such an orbit may expand to reach a second equilibrium configuration which is stable, or it may decay until the two stars coalesce. The present problem, however is likely to be substantially more complicated because Krzeminski's star is losing mass, and as it evolves, its radius and internal structure will change. In order to determine the stability of the Cen X-3 orbit against tidal decay, one would have to integrate the coupled differential equations of motion (eqs. [6a] and [6b]) for an assumed (and highly uncertain) evolution of Krzeminski's star under the influence of its nuclear evolution and mass loss. All that we can say at this point is that its high moment of inertia, in relation to that of the orbit, makes it a good candidate for tidal instability.

If the orbit of Cen X-3 is in fact unstable, the question then arises as to how such a state could be achieved. Since the orbit is presently observed to be highly circular, it was presumably stable at some previous epoch, at least for a period of time comparable to the circularization time scale at that epoch. A likely possibility is that the evolutionary expansion of Krzeminski's star resulted in an increase in its moment of inertia to a value exceeding the critical value of one-third that of the orbital moment of inertia.

Finally, another potentially very important conclusion can be drawn from the observed decreases in the orbital period of Cen X-3. From the fact that the total mass of the binary system can only decrease with time, we can infer from Kepler's third law that the orbital separation must also be decreasing with time. We further note that the mass ratio, $q \equiv M_x/M_c$, can only increase with time. If Krzeminski's star is in corotation with the orbit, it then follows that its Roche lobe, R_L, is shrinking at a rate $\dot{R}_L/R_L \gtrsim 1.2\times10^{-6}\ {\rm yr}^{-1}$. Furthermore, for all reasonable rotation rates, the actual critical potential lobe of Krzeminski's star will also be decreasing unless the rotation rate of the star is decreasing at least a factor of ~ 3 faster than the orbital period is decaying (Pratt-Strittmatter 1976 effect). It therefore seems highly likely that the critical potential lobe of Krzeminski's star is shrinking at a fractional rate of at least $1.2\times10^{-6}\ {\rm yr}^{-1}$. If this is the case, one of the following situations should apply: (i) Krzeminski's star and its atmosphere are smaller than the critical potential lobe and the mass transfer takes place via a stellar wind (see above discussion). (ii) The critical potential lobe is within a few atmospheric scale heights of the photosphere, and mass transfer proceeds via Roche lobe overflow (Savonije 1979, 1980). In this case the star may even by expanding at the natural rate governed by its nuclear evolution ($\dot{R}_c/R_c \approx 2\times10^{-7}\ {\rm yr}^{-1}$; see Savonije 1979; van der Linden 1981), with the mass transfer rate increasing as the critical potential lobe penetrates further into the stellar atmosphere. We would then be observing a period of relatively controlled mass transfer ($\lesssim 3\times10^{-8}\ M_\odot\ {\rm yr}^{-1}$) to be followed in $\sim 10^4$ yr by catastrophic mass transfer on a thermal time scale (see Savonije 1980, 1982). If this is the case, then the rate of shrinking of the critical potential lobe may be very important in governing the lifetime of the X-ray source. (iii) Krzeminski's star is shrinking at a rate equal to that

© American Astronomical Society • Provided by the NASA Astrophysics Data System

1983ApJ...268..790K

at which the critical potential lobe is shrinking. This should not be the case during the normal evolution of an O star after leaving the zero-age main sequence, except during core contraction following core hydrogen exhaustion (van der Linden 1981), or unless there are large *transient* episodes of mass loss ($\gtrsim 10^{-5}\ M_\odot\ \mathrm{yr}^{-1}$; Savonije, van den Heuvel, and Takens 1981).

In summary, we have determined the mean rate of decrease in the orbital period of Cen X-3 to be $\dot{P}_{\rm orb}/P_{\rm orb} = -(1.8 \pm 0.1) \times 10^{-6}\ \mathrm{yr}^{-1}$; this is about one-fourth the previously reported value (Fabbiano and Schreier 1977) and is more statistically significant. The overall long-term period decrease can be well accounted for by tidal interaction between Krzeminski's star and the orbiting neutron star.

The authors are grateful to P. Hut, P. C. Joss, S. Tremaine, E. P. J. van den Heuvel, and J.-P. Zahn for helpful discussions, and to P. Goetz for assistance with the data analysis. We also thank T. Dobson for her work in preparing the manuscript.

REFERENCES

Abbott, D. C., Bieging, J. H., Churchwell, E., and Cassinelli, J. P. 1980, *Ap. J.*, **238**, 196.
Avni, Y., and Bahcall, J. N. 1974, *Ap. J.* (*Letters*), **192**, L139.
Bahcall, J. N. 1978, *Ann. Rev. Astr. Ap.*, **16**, 241.
Bonnet-Bidaud, J. M., and van der Klis, M. 1979, *Astr. Ap.*, **73**, 90.
Buff, J., *et al.* 1977, *Ap. J.*, **212**, 768.
Chevalier, R. A. 1975, *Ap. J.*, **199**, 189.
Counselman, C. C. 1973, *Ap. J.*, **180**, 307.
Darwin, G. H. 1879, *Proc. Roy. Soc. London*, **29**, 168.
Davidson, K., and Ostriker, J. P. 1973, *Ap. J.*, **179**, 585.
Deeter, J. E., Boynton, P. E., and Pravdo, S. H. 1981, *Ap. J.*, **247**, 1003.
Fabbiano, G., and Schreier, E. J. 1977, *Ap. J.*, **214**, 235.
Garmany, C. D., Olson, G. L., Conti, P. S., and van Steenberg, M. E. 1981. *Ap. J.*, **250**, 660.
Ghosh, P., and Lamb, F. K. 1979, *Ap. J.*, **234**, 296.
Giacconi, R. 1975, *Ann. NY Acad. Sci.*, **262**, 312.
Gursky, H., and Schreier, E. 1975, in *Neutron Stars, Black Holes and Binary X-ray Sources*, ed. H. Gursky and R. Ruffini (Dordrecht: Reidel), p. 175.
Howe, S. K., *et al.* 1982, *Ap. J.*, submitted.
Hut, P. 1980, *Astr. Ap.*, **92**, 167.
_____. 1981, *Astr. Ap.*, **99**, 126.
Hutchings, J. B., Cowley, A. P., Crampton, D., van Paradijs, J., and White, N. E. 1979, *Ap. J.*, **229**, 1079.
Jackson, J. C. 1975, *M.N.R.A.S.*, **172**, 483.
Kelley, R., Rappaport, S., and Petre, R. 1980, *Ap. J.*, **238**, 699.
Krzeminski, W. 1974, *Ap. J.* (*Letters*), **192**, L135.
Lamb, F. K., Pethick, C. J., and Pines, D. 1973, *Ap. J.*, **184**, 271.
Lamers, H. J. G. L. M. 1981, *Ap. J.*, **245**, 593.
Lamers, H. J. G. L. M., van den Heuvel, E. P. J., and Petterson, J. A. 1976, *Astr. Ap.*, **49**, 327.
Lecar, M., Wheeler, J. C., and McKee, C. F. 1976, *Ap. J.*, **205**, 556.
Murakami, T., *et al.* 1982, *Ap. J.*, in press.
Nicholson, P. D. 1979, Ph.D. thesis, California Institute of Technology.
Pounds, K. A., Cooke, B. A., Ricketts, M. J., Turner, M. J., and Elvis, M. 1975, *M.N.R.A.S.*, **172**, 473.
Pratt, J. P., and Strittmatter, P. A. 1976, *Ap. J.* (*Letters*), **204**, L29.
Primini, F., Rappaport, S., and Joss, P. C. 1977, *Ap. J.*, **217**, 543.
Pringle, J. E., and Rees, M. J. 1972, *Astr. Ap.*, **21**, 1.
Rappaport, S., and Joss, P. C. 1977, *Nature*, **266**, 683.
_____. 1981, in *X-Ray Astronomy with the Einstein Satellite*, ed. R. Giacconi, (Dordrecht: Reidel), p. 123.
_____. 1982, in *Accretion Driven Stellar X-Ray Sources*, ed. W. H. G. Lewin and E. P. J. van den Heuvel (Cambridge: Cambridge University Press), in press.
Rappaport, S., Joss, P. C., and McClintock, J. E. 1976, *Ap. J.* (*Letters*), **206**, L103.
Rappaport, S., Joss, P. C., and Stothers, R. 1980, *Ap. J.*, **235**, 570.
Savonije, G. J. 1979, *Astr. Ap.*, **71**, 352.
_____. 1980, *Astr. Ap.*, **81**, 25.
_____. 1982, in *Accretion Driven Stellar X-Ray Sources*, ed. W. H. G. Lewin and E. P. J. van den Heuvel (Cambridge: Cambridge University Press), in press.
Savonije, G. J., van den Heuvel, E. P. J., and Takens, R. 1981, private communication.
Schreier, E. J., and Fabbiano, G. 1976, in *X-Ray Binaries* (NASA SP-389), p. 197.
Schreier, E., Giacconi, R., Gursky, H., Kellogg, E., Levinson, R., and Tananbaum, H. 1973, *IAU Circ.*, No. 2524.
Schreier, E., Levinson, R., Gursky, H., Kellogg, E., Tananbaum, H., and Giacconi, R. 1972, *Ap. J.* (*Letters*), **172**, L79.
Schreier, E. J., Swartz, K., Giacconi, R., Fabbiano, G., and Morin, J. 1976, *Ap. J.*, **204**, 539.
Sparks, W. M. 1975, *Ap. J.*, **199**, 462.
Stothers, R. 1982, private communication.
Thomas, H.-C. 1974, *Ap. J.* (*Letters*), **191**, L25.
_____. 1977, *Ann. Rev. Astr. Ap.*, **15**, 127.
Tuohy, I. R. 1976, *M.N.R.A.S.*, **174**, 45p.
van den Heuvel, E. P. J., and de Loore, C. 1973, *Nature*, **245**, 117.
van der Klis, M., Bonnet-Bidaud, J. M., and Robba, N. R. 1980, *Astr. Ap.*, **88**, 8.
van der Linden, T. 1981, private communication.
van Hamme, W. 1979, *Ap. Space Sci.*, **64**, 239.
Wheeler, J. C., McKee, C. F., and Lecar, M. 1974, *Ap. J.* (*Letters*), **192**, L71.
Zahn, J.-P. 1975, *Astr. Ap.*, **41**, 329.
_____. 1977, *Astr. Ap.*, **57**, 383.

G. W. CLARK and S. RAPPAPORT: Center for Space Research, Massachusetts Institute of Technology, Cambridge, MA 02139

R. L. KELLEY: NASA Goddard Space Flight Center, Code 661, Greeenbelt, MD 20771

L. D. PETRO: Atmospheric and Environmental Research, 840 Memorial Drive, Cambridge, MA 02139

© American Astronomical Society • Provided by the NASA Astrophysics Data System